Z. Phys. Chem. **220** (2006) 1595–1608 / **DOI** 10.1524/zpch.2006.220.12.1595

Formation of Perfluorobutene-2 Epoxide in the Thermal Gas-Phase Reaction of Perfluorobutene-2 with Nitrogen Dioxide. An Experimental and DFT Study

By J. Czarnowski and C. J. Cobos*

Instituto de Investigaciones Fisicoquímicas Teóricas y Aplicadas (INIFTA), Departamento de Química, Facultad de Ciencias Exactas, Universidad Nacional de La Plata, CONICET, CICPBA, Casilla de Correo 16, Sucursal 4, (1900) La Plata, Argentina

(Received September 20, 2006; accepted September 20, 2006)

Thermal Reaction of Perfluorobutene-2 with NO_2 / Perfluorobutene-2 Epoxide / DFT Calculations

The mechanism of the thermal reaction between perfluorobutene-2 and NO_2 in the gas phase has been investigated in the temperature range 418.5–470.0 K. At temperatures below 432 K, equal amounts of perfluorobutene-2 epoxide (PFBE) and NO are formed. At higher temperatures, PFBE decomposes generating $CF_3C(O)F$ and CF_3CF biradicals. The latter self-recombine reforming the parent perfluorobutene-2 molecule. The addition of O_2 does not affect the reaction course. This reaction system provides a new and promising method for PFBE preparation. Based on the perfluorobutene-2 consumption, PFBE yields larger than 90% were obtained. The energetics of the relevant reaction pathways has been calculated using various density functional theory methods. These calculations confirm the reaction mechanism based on experimental results. The computed vibrational spectra predicted for the PFBE at the B3LYP/6-311+G(3df) and B98/6-311+G(3df) levels of theory are in very good agreement with that obtained experimentally.

1. Introduction

The addition reactions of NO_2 to halogenated olefins have been subject of several studies [1–8]. These reactions are generally employed for preparative purposes, because NO_2 can act either as nitrating or as oxidating agent depending on the character of the atoms linked to the olefinic carbons. The major products in these systems are vicinal dinitro compounds, nitrohaloacetyl

* Corresponding author. E-mail: cobos@inifta.unlp.edu.ar

halides, nitroketones and NOX (X = Cl or F). From a mechanistic point of view these processes are interpreted by using free radical reaction schemes initiated by the N-attack on the olefinic C atom. As several reaction channels may be possible, the elucidation of the mechanism of these reactions is important for organic and inorganic chemistry.

Detailed mechanistic studies, kinetics parameters and product formation have been reported for several gas-phase reactions of NO_2 with perhalogenated ethenes CF_2CX_2, where X = F, Br or Cl, at temperatures ranging from about 300 to 430 K [9–12]. A basic common mechanism for these reactions can be postulated as follows:

$$NO_2 + CF_2CX_2 \rightarrow CF_2(NO_2)CX_2^{\bullet}$$
$$CF_2(NO_2)CX_2^{\bullet} + NO_2 + M \rightarrow CF_2(NO_2)CX_2NO_2 + M$$
$$CF_2(NO_2)CX_2^{\bullet} + NO_2 \rightarrow CF_2(NO_2)C(O)X + XNO\,.$$

In the reaction of NO_2 with CF_2CF_2, $CF_2(NO_2)C(O)F$ and FNO are formed [9]. The nitration of CF_2CFBr leads to the formation of $CF_2(NO_2)C(O)F$, $CF_2(NO_2)CFBr(NO_2)$ and BrNO, which is in equilibrium with Br_2 and NO [10]. The addition of NO_2 to CF_2CFCl gives as final products $CF_2(NO_2)C(O)F$, ClNO and $CF_2(NO_2)CFCl(NO_2)$ [11] and $CF_2(NO_2)C(O)Cl$, ClNO and $CF_2(NO_2)CCl_2(NO_2)$ are generated in the thermal reaction of NO_2 with CF_2CCl_2 [12]. The reaction of NO_2 with CF_3CFCF_2 at 413–433 K, follows a different pattern, giving mostly perfluoropropene epoxide, C_3F_6O, and NO [13], $CF_3CF(NO_2)CF_2(NO_2)$ and nitroperfluoroacetone being also formed, though in smaller quantities. The following mechanism was postulated for this reaction:

$$CF_3CF{=}CF_2 + NO_2 \rightarrow CF_3C^{\bullet}FCF_2NO_2$$

$$CF_3C^{\bullet}FCF_2NO_2 \rightarrow CF_3\underset{\diagdown\,\diagup}{CF}{-}CF_2 + NO$$
$$CF_3C^{\bullet}FCF_2NO_2 + NO_2 + M \rightarrow CF_3CF(NO_2)CF_2NO_2 + M$$
$$CF_3C^{\bullet}FCF_2NO_2 + NO_2 \rightarrow CF_3C(O)CF_2NO_2 + FNO\,.$$

The absence of $CF_3C(O)F$ in this reaction suggests that C_3F_6O does not decompose appreciably below 433 K. It has been reported that, in the temperature range 463–503 K, C_3F_6O decomposes unimolecularly to give $CF_3C(O)F$ and the biradical difluorocarbene, CF_2 [14, 15]. In addition to $CF_3C(O)F$, the major product of this pyrolysis is C_2F_4 produced by dimerization of CF_2 biradicals. Perfluorocyclopropane is also formed by addition of CF_2 to CF_2CF_2.

Continuing our studies on the nitration of perhalogenated olefins, in the present work the reaction between perfluorobutene-2, C_4F_8-2 and NO_2, was investigated in the temperature range 418.5–470.0 K. The experiments were

complemented with quantum chemical calculations at various density functional theory (DFT) levels to clarify relevant features of the potential energy surface of this reaction.

2. Experimental technique

The experimental setup has been described elsewhere [10–13]. Therefore, only a brief description is presented here. The experiments were performed measuring the total pressure at constant volume and temperature in a conventional static vacuum system free from moisture and grease. The employed spherical quartz reaction vessel (270 cm^3) is connected to a sensitive quartz spiral gauge used as a null instrument and to a mercury manometer (± 0.02 Torr). The temperature of the reaction cell was maintained constant within ± 0.1 K by means of a Lauda thermostat filled with a Dow Corning 200/300 Fluid. The infrared spectra were recorded on a Shimadzu IR-435 spectrophotometer, using a 10 cm long Pyrex cell, fitted with NaCl windows.

All commercial reactants were purified. C_4F_8-2 (PCR, 97–98%), was repeatedly trap-to-trap distilled at low-pressure, the middle fraction being retained each time. Small amounts of NO present in NO_2 (Matheson 99.5%) were eliminated by a series of freeze-pump-thaw cycles in presence of O_2 until the blue colour due to the formation of N_2O_3 disappeared. The degassed NO_2 was purified by fractional condensation using the fraction that distilled between 213 and 243 K. O_2 (La Oxígena 99.9%) was bubbled through 98% analytical grade H_2SO_4, passed slowly through a Pyrex glass coil maintained at 153 K and stored in a Pyrex flask.

The experiments were carried out at 418.5, 432.4, 454.0, 463.0 and 470.0 K. The initial pressure of C_4F_8-2 was varied between 39.3 and 203.7 Torr, that of NO_2 between 11.1 and 210.4 Torr and that of O_2 between 81.4 and 125.8 Torr.

3. Results and discussion

3.1 Reaction mechanism for C_4F_8-2 + NO_2

At the lowest temperature studied, 418.5 K, no changes in the total pressure were observed. However, in addition to the non-consumed reactants, the products perfluorobutene-2 epoxide, C_4F_8O (PFBE), and NO were observed in the reaction mixture. The PFBE was identified by its infrared spectrum. The absorption band located at 1504 cm^{-1} and assigned to the ring-breathing mode is very well reproduced by the quantum chemical calculations described in the next section. This fundamental mode, characteristic of fluorinated olefin epoxides, is not present in other fluorinated compounds [16]. This band appears at 1551 cm^{-1} for perfluoropropene epoxide [13], at 1500 cm^{-1} for 1,1-dichloro-

Table 1. Experimental data for the thermal reaction between C_4F_8-2 and NO_2. Δp indicates the increase of the total pressure during the reaction time Δt.

T (K)	Δt (min)	Δp (Torr)	C_4F_8-2 (Torr)	NO_2 (Torr)	$O_{2,\text{initial}}$ (Torr)	$O_{2,\text{final}}$ (Torr)	PFBE (Torr)	$CF_3C(O)OF$ (Torr)
418.5	301.3	–	100.0	11.1	–	–	6.7	–
432.4	306.0	2.0	39.9	198.5	–	–	36.6	4.0
432.4	181.5	–	39.3	12.1	81.4	81.2	2.5	–
432.4	294.0	2.2	199.3	42.4			37.1	4.0
432.4	210.0	1.0	101.6	40.0	125.8	125.6	18.0	2.0
455.0	258.7	2.4	203.6	39.1	–	–	35.6	4.8
455.0	249.8	2.5	41.9	208.8	–	–	37.6	5.0
463.0	2340.0	8.2	42.3	210.4	–	–	33.9	16.4
470.0	243.0	3.5	203.7	47.6	–	–	43.0	7.0

2,2-difluoroethene epoxide [17], at 1545 cm^{-1} for chlorotrifluoroethene epoxide [17] and at 1540 cm^{-1} for bromotrifluoroethene epoxide [18].

The above findings are consistent with the overall reaction

$$C_4F_8\text{-}2 + NO_2 \rightarrow C_4F_8O + NO \qquad \Delta n = 0\,, \tag{I}$$

which occurs without change in the total number of moles and, therefore, without change in total pressure. In the temperature range 432.4–470.0 K, a significant increase of pressure was observed. Under these conditions, in addition to PFBE and NO, the formation of $CF_3C(O)F$ was detected by its infrared absorption band located at 1897 cm^{-1} [19, 20]. The total reaction in this temperature range can be described by the stoichiometric equation:

$$2C_4F_8\text{-}2 + 3NO_2 \rightarrow C_4F_8O + 3NO + 2CF_3C(O)F \qquad \Delta n = 1\,. \tag{II}$$

Representative experimental data are listed in Table 1. Here, Δp denotes the increase in total pressure corresponding to a reaction time of Δt. According to Eq. (II), the pressure of the formed $CF_3C(O)F$ is equal to $2\Delta p$.

In order to quantify the amount of PBFE produced, an IR calibration curve was constructed. For this, pure PFBE was prepared at 463.0 K by allowing to react the mixture of 42.3 Torr of C_4F_8-2 and 210.4 Torr of NO_2 during 39 h to achieve the total consumption of C_4F_8-2. Afterwards, the gaseous mixture was cooled to a room temperature of 298 K and then 111.1 Torr of O_2 were added to convert the formed NO into NO_2. Subsequently, the reaction vessel was rapidly cooled to liquid nitrogen temperature and O_2 evacuated. The remaining reaction mixture was separated by fractional condensation. The fraction volatile at 153 K consisted of $CF_3C(O)F$. Pure PFBE was separated between 153 and 173 K and NO_2 remained as condensed residue at 173 K.

The obtained pure PFBE was employed to draw the plot depicted in Fig. 1. The selected infrared band located at 1504 cm^{-1} is not interfered by other

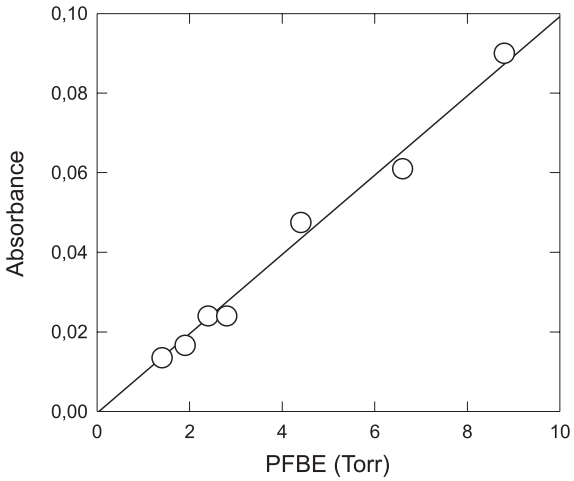

Fig. 1. Plot of the absorbance at 1504 cm^{-1} as a function of PFBE pressure. The straight line is the result of a least-squares fit (see text).

bands. The linearity of the plot indicates that the Beer–Lambert law is clearly obeyed under the present conditions. Therefore, a reliable absorption cross-section for PFBE at 298 K can be determined from the slope. The obtained value is $(3.1 \pm 0.2) \times 10^{-20}$ cm^2 $molecule^{-1}$. This small value is consistent with the low intensity observed experimentally and predicted computationally (see the next section) for this band. This calibration allowed us to determine the PFBE pressures corresponding to the experiments given in Table 1.

The absence of pressure change below 432 K and the similar vapour pressure values for C_4F_8-2 and PFBE which exclude their separation by fractional condensation, make impracticable a kinetic study similar to those performed for other olefins [9–13]. Therefore, the reaction mechanism was inferred from the observed reaction products and previously related studies. The proposed reaction scheme is supported by the detailed quantum chemical calculations presented below.

By contrast to the nitration reactions of CF_2CYX (X = Cl or Br and Y = Cl or F) in presence of O_2 [21, 22], the addition of O_2 to the system C_4F_8-2 + NO_2 does not affect the course of this reaction, as shown in Table 1. The oxidation of CF_2CYX ethylenes has been explained by the following initial reaction sequence:

$$CF_2CYX + NO_2 \rightarrow CF_2(NO_2)CYX^{\bullet}$$
$$CF_2(NO_2)CYX^{\bullet} + O_2 + M \rightarrow CF_2(NO_2)CYXO_2^{\bullet} + M$$
$$2CF_2(NO_2)CYXO_2^{\bullet} \rightarrow 2CF_2(NO_2)CYXO^{\bullet} + O_2$$
$$CF_2(NO_2)CYXO^{\bullet} \rightarrow CF_2(NO_2)C(O)Y + X\,.$$

The X atoms, adding in presence of O_2 to the double bond, initiate the chain reaction leading to the formation of the oxidation products. The major final products for $CF_2CCl_2 + NO_2 + O_2$ are $CF_2ClC(O)Cl$, F_2CO and Cl_2CO [21] and those for $CF_2CFBr + NO_2 + O_2$ are $CF_2BrC(O)F$, F_2CO and FBrCO [22]. In both reactions very small amounts of $CF_2(NO_2)C(O)Cl$ and $CF_2(NO_2)C(O)F$ are also formed, respectively. Therefore, the nitration of the halogenated ethenes in the presence of O_2 generates reaction products different from those observed in the C_4F_8-2/NO_2/O_2 system.

The above considerations indicate that the $CF_3CF(NO_2)CFCF_3$ radical is not formed in the initial step or, more probably, presents a lifetime too short to be stabilized which precludes its reaction with O_2. This will be analyzed in the next section.

It appears interesting to compare the present system with the oxidation of C_4F_8-2 at 323–352 K initiated and propagated by CF_3O radicals generated by F atom abstraction from CF_3OF by C_4F_8-2 [23]. Here, $CF_3OC(O)F$ and $CF_3C(O)F$ are the main products and no formation of perfluorobutene-2 epoxide has been observed. All the experimental results were very well rationalized by a chain reaction mechanism in which a C–C bond of the intermediate radical $CF_3OCF(CF_3)C(O)FCF_3$ is broken. In particular, the $CF_3C(O)F$ is generated in the following way:

$$CF_3O^\bullet + C_4F_8\text{-}2 \rightarrow CF_3OCF(CF_3)C^\bullet FCF_3$$
$$CF_3OCF(CF_3)C^\bullet FCF_3 + O_2 + M \rightarrow CF_3OCF(CF_3)C(O_2)^\bullet FCF_3 + M$$
$$2CF_3OCF(CF_3)C(O_2)^\bullet FCF_3 \rightarrow 2CF_3OCF(CF_3)C(O)^\bullet FCF_3 + O_2$$
$$CF_3OCF(CF_3)C(O)^\bullet FCF_3 \rightarrow CF_3C(O)F + CF_3OC^\bullet F(CF_3)\,.$$

The $CF_3OC^\bullet F(CF_3)$ radicals then recombine with O_2 to form $CF_3OC(O_2)^\bullet F(CF_3)$ radicals which generate $CF_3OC(O)^\bullet F(CF_3)$ by self-reaction. This species undergoes unimolecular C–C bond scission to form the other reaction product $CF_3OC(O)F$ and CF_3 radicals. The latter add to O_2 forming CF_3O_2 radicals which subsequently regenerate the chain propagating species CF_3O by self-reaction.

The lack of O_2 effect on the reaction C_4F_8-2 + NO_2 shows that in this system the $CF_3CF(NO_2)CFCF_3$ radical is not stabilized. Then, due to the fact that $CF_3C(O)F$ is also formed in absence of O_2, it can be assumed that this compound is formed through a reaction mechanism different from that postulated to interpret the C_4F_8-2 + CF_3O system.

As below 432.4 K the only product formed is perfluorobutene-2 epoxide, the following primary step is proposed:

$$C_4F_8\text{-}2 + NO_2 \rightarrow CF_3\overset{\displaystyle O\text{—}NO}{\overset{|\quad|}{C}}F\text{—}CFCF_3 \rightarrow CF_3\overset{\displaystyle O}{\overset{/\ \backslash}{C}}F\text{—}CFCF_3 + NO \qquad (1)$$

An analogous four-member ring intermediate was employed to explain the formation of C_3F_6O in the thermal reaction of C_3F_6 with NO_2 [13]. As shown in Table 1, at temperatures above 432 K a pressure increase was measured and the concomitant formation of $CF_3C(O)F$ is evidenced. To explain this, we assume an unimolecular pathway in which a concerted C–C and C–O bond cleavage generates $CF_3C(O)F$ and fluoro(perfluoromethyl)carbene, CF_3CF:

$$CF_3\overset{\overset{O}{\diagup\diagdown}}{C}F-CFCF_3 \rightarrow CF_3C(O)F + CF_3CF: \qquad (2)$$

A related process has been proposed to interpret the thermal cracking of C_3F_6O into $CF_3C(O)F$ and singlet CF_2 [14]. Taking into account the molecular complexity of PFBE, reaction (2) is probably, under the present conditions, very close to the high pressure limit. The CF_3CF generated in reaction (2), afterwards recombine reforming the parent C_4F_8-2,

$$CF_3CF: + CF_3CF: + M \rightarrow C_4F_8\text{-}2 + M \qquad (3)$$

This process has been proposed in the mechanism of the pyrolysis of $CF_3CF_2SiF_3$ to give the products SiF_4 and C_4F_8-2 above 433 K [24]. In addition, this work shows that CF_3CF does not add to the double bond of C_4F_8-2, probably due to steric hindrance effects. This effect is corroborated by the fact that the reactivity of FNO with C_2F_4 is much higher than with C_4F_8-2 [25]. The latter reaction required temperatures above 523 K.

The obtained results indicate that the reaction between C_4F_8-2 with NO_2 provides a new and simple method for PFBE preparation. An analysis of the data of Table 1 based on consumed C_4F_8-2, leads to a PFBE yield larger than 90%. For comparison, a C_3F_6O yield of 63–89% is obtained in the reaction of C_3F_6 with NO_2 at 413–433 K [13]. The PFBE has been also synthesized by passing at room temperature a stream of C_4F_8-2 gas through a solution of potassium hydroxide in water and a mixture of hydrogen peroxide and methanol [16]. More recently, a number of epoxides have been prepared with yields ranging from 69 to 94% treating perfluorinated alkenes with $M(OX)_n$ (M=Na, K, Ba, Ca and X=Cl, Br, being $n = 1, 2$) [26].

3.2 Density functional theory calculations

We present here the results obtained from a theoretical study of the mechanism of the thermal reaction between C_4F_8-2 and NO_2. The popular hybrid B3LYP density functional of the DFT was used to compute fully optimized geometries of the reactants, products, various intermediates and transition states using analytical gradient methods. Harmonic vibrational frequencies employed to make zero-point energy corrections (ZPE) and to characterize the nature of the stationary points have been calculated *via* analytical second derivates methods.

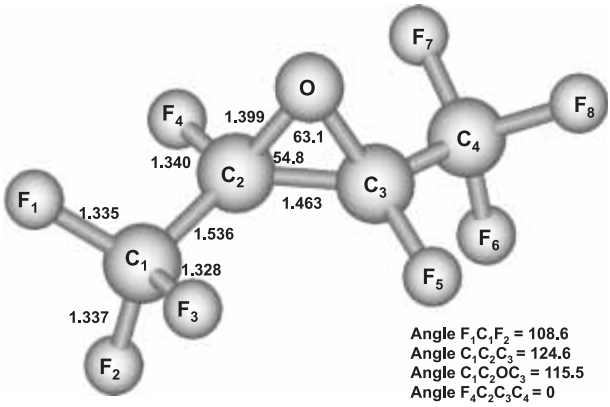

Fig. 2. Optimized geometry (in Å and degrees) for PFBE computed at the B3LYP/6-311+G(3df) level of theory.

The intermediates were characterized by all the real frequencies, and the transition states, as confirmed by normal-mode analysis, present only one imaginary frequency. The B3LYP approach employs the Becke's three-parameter nonlocal exchange functional [27] coupled to the nonlocal correlational functional of Lee, Yang and Parr [28]. The standard 6-31G(d) split-valence Pople's basis set was employed for this calculations [29]. The derived vibrational frequencies were scaled by a standard factor of 0.96 [30]. To improve total energies, single-point energy calculations with the extended 6-311+G(3df) triple split valence basis set [29] were then performed (B3LYP/6-311+G(3df)//B3LYP/6-31G(d)). The particular contributions of exchange and correlation functionals that will give the best results in a given instance are difficult to predict. For this reason, as in recent works from this laboratory [31–35], we have employed several combination of them. In this way, the recent DFT formulations B98 [36], B97-2 [37], B1B95 [38] and O3LYP [39] were also used in the single-point computations. As a measure of the spin contamination in these calculations, the expectation value of the $\langle S^2 \rangle$ operator was not greater than 0.76, close to the exact value of 0.75 for doublet states. The uncertainties in the methods employed allow to get an error estimate of about ± 3 kcal mol^{-1} in the energetics [40]. We cannot afford for the present fifteen heavy atoms system more accurate and demanding computations such as provided by high level composite *ab initio* model chemistries [41]. All calculations were carried out with the Gaussian 03 program package with default integration grids [42].

Figure 2 shows the B3LYP/6-311+G(3df) optimized structure for PFBE. Mean bond distances and angles differing respectively in only 0.007 Å and 0.15 degrees were computed at the B98/6-311+G(3df) level. For the sake of simplicity they have not been reported here. In these calculations the 104 valence electrons of PFBE were accommodated in molecular orbitals which

Table 2. Harmonic vibrational frequencies (in cm^{-1}), infrared intensities (in $km\,mol^{-1}$) and mode description for PFBE.

experimental		B3LYP/6-311+G(3df)		B98/6-311+G(3df)		assignment
frequency	I_{rel}	frequency	intensity[a]	frequency	intensity[a]	
1504	4	1507	25 (4)	1508	26 (4)	C_2C_3 stretch
1367	7	1353	32 (5)	1368	31 (5)	C_1C_2 s-stretch
1321	68	1293	307 (48)	1303	333 (53)	C_1C_2 a-stretch
1250	100	1229	643 (100)	1252	628 (100)	CF_3 a-stretch
–	–	1211	138 (21)	1234	138 (22)	–
1217	80	1185	325 (51)	1207	339 (54)	CF_3 s-stretch
–	–	1179	26 (4)	1201	27 (4)	–
1163	30	1148	107 (17)	1169	121 (19)	CF a-stretch
1117	19	1124	96 (15)	1130	66 (11)	COC deformation
1092	9	1092	19 (3)	1093	38 (6)	CCCC deformation
950	37	951	212 (33)	955	206 (33)	COC a-stretch
–	–	812	2 (0.3)	812	0.6 (0.1)	–
–	–	765	0.1 (0.02)	773	0.07 (0.01)	–
717	10	731	74 (11)	737	79 (13)	CF_3 bend
–	–	635	2	639	2	–
–	–	608	14	613	13	–
–	–	587	0.6	592	0.8	–
–	–	579	4	585	4	–
–	–	529	4	534	4	–
–	–	524	6	530	7	–
–	–	438	1	440	1	–
–	–	428	0.7	431	0.6	–
–	–	397	0.4	398	0.4	–
–	–	329	0.6	331	0.7	–
–	–	293	0.9	293	0.9	–
–	–	279	4	280	4	–
–	–	267	0.7	267	0.6	–
–	–	232	0.5	231	0.5	–
–	–	195	0.007	192	0.01	–
–	–	119	0.7	118	0.7	–
–	–	83	0.5	83	0.5	–
–	–	51	0.2	51	0.2	–
–	–	35	0.07	36	0.07	

[a] Relative intensity values (I_{rel}) in parentheses.

comprise 507 basis functions based on 754 primitive Gaussians. In addition, calculations carried out at the more modest B3LYP/6-31G(d) level (195 basis functions and 364 primitive Gaussians) only differ in 0.003 Å and in 0.26 degrees from those computed at the B3LYP/6-311+G(3df) level. These small differences between the two levels of calculations justify the single-point energy calculations given below. Unscaled harmonic vibrational frequencies, infrared intensities and approximate mode assignations are listed in Table 2.

Mode assignations were derived from the animation of the normal modes corresponding to the fundamental vibrational frequencies. Several of the modes are significantly mixed and therefore the consigned assignations are only approximated. A comparison between the experimental frequencies and those estimated with the B3LYP and B98 approaches led to mean absolute deviations of 14 and 8 cm^{-1} respectively. At the same levels of theory, the deviations in the relative infrared intensities are of only 8 and 7%. The very good agreement found between the experimental and estimated parameters supports the presence of PFBE in the system.

The total energy of the reactants C_4F_8-2 + NO_2 and the relative energies (both with ZPE corrections) for the relevant species computed at the different levels of theory are compiled in Table 3. Due to fact that the real exchange-correlation functional remains unknown (Hohenberg–Kohn theorem [43]), a significant difference in the relative energies is appreciable. However, all calculations predict similar potential energy features. The calculated reaction pathways on the basis of the structural evolutions are shown in Fig. 3. Other channels are discarded because of their high endothermicities. In Fig. 3 the total energy for C_4F_8-2 + NO_2 is set as zero. The indicated relative energies are the average values resulting from all quantum chemical calculations listed in Table 3. The C_4F_8-2 + NO_2 reaction starts by the formation of a C_4F_8–NO_2 transition state (TS1) which generates the nitro radical $CF_3CF(NO_2)CFCF_3$ (denoted as $C_4F_8NO_2$). This N-addition can find support from spin distribution analysis. In fact, at the B3LYP/6-311+G(3df) level, the spin density of NO_2 radical is 0.528*e* on N atom and 0.236*e* on O atoms. The N atom with the larger spin density should be the most reactive site. This finding is consistent with the above discussed nitration reactions where the nitro radicals are stabilized. The calculations give a transition state with a C–N bond length of 1.979 Å and one imaginary frequency of 407i cm^{-1}. The mean electronic barrier for TS1 is 17.4 ± 1.3 kcal mol^{-1}. From this value an activation energy of $E_{a,\infty} = \Delta H^{0\#} + 2RT = 19.2$ kcal mol^{-1} can be estimated for the NO_2 addition to C_4F_8-2 at 450 K. For comparison, values of 7.5, 10.9, 10.8 and 10.5 kcal mol^{-1} have been respectively reported for the ethylenes CF_2CF_2 [9], CF_2CFBr [10], CF_2CFCl [11] and CF_2CCl_2 [12]. A larger value of (15.4 ± 1.2) kcal mol^{-1} has been recently measured for the nitration of the larger olefin C_3F_6 [13]. These results together with the present estimation for C_4F_8-2 suggest that the activation energy of nitration reactions increases with the number of C atoms in the olefin. After forming, the vibrationally excited $C_4F_8NO_2$ adduct can either be collisionally stabilized or more probably, due to the small exit barrier mostly attributed to the internal rotation around the formed N–C bond (TS2), undergo an intramolecular rearrangement generating the vibrationally excited four-center radical c-$C_4F_8NO_2$ indicated in reaction (1). This fast step is responsible for the short life of the $C_4F_8NO_2$ intermediate and justifies the lack of nitroderivated compounds in the present system. The reaction proceeds *via* decomposition of the energized

Table 3. Computed total and relative energies of reactants, intermediates, transition states (TS) and products for the reaction of C_4F_8 with NO_2 at different DFT levels with B3LYP/6-31G(d) optimized geometries. The total energies are in units of a.u., and the relative energies (including scaled ZPE corrections) are in units of kcal mol^{-1}.

species	ZPE	B3LYP/ 6-311+G(3df)	B1B95/ 6-311+G(3df)	B98/ 6-311+G(3df)	B97-2/ 6-311+G(3df)	O3LYP/ 6-311+G(3df)
$C_4F_8 + NO_2$	33.5	−1156.579459	−1156.291568	−1156.178771	−1156.215818	−1156.224778
$C_4F_8NO_2$	35.4	14.0	12.0	11.1	13.1	17.5
c-$C_4F_8NO_2$	35.8	1.6	−3.0	−3.3	0.0	5.3
PBFE + NO	33.6	−19.7	−25.3	−21.6	−21.6	−17.6
$CF_3C(O)F + CF_3CF$	27.7	31.5	34.5	31.6	34.8	35.0
TS1	34.1	17.5	17.4	15.7	17.1	19.3
TS2	35.3	17.3	15.3	14.4	16.4	21.3
TS3	33.4	19.2	21.4	17.4	21.5	23.7
TS4	28.4	31.7	33.9	31.0	35.6	38.3

c-$C_4F_8NO_2$ through a TS3 transition state, located at about 20 kcal mol^{-1} above the C_4F_8-2 + NO_2 asymptote, giving the experimentally observed C_4F_8O and NO after thermalization. Therefore, the present potential energy scheme

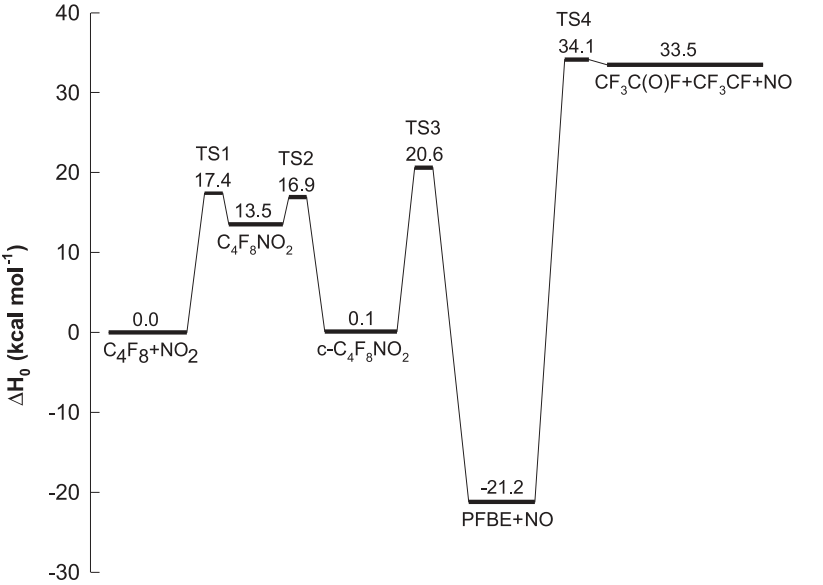

Fig. 3. Schematic representation of the potential energy surface for the C_4F_8-2 + NO_2 reaction. The indicated energies are average DFT values (see text).

agrees with the sequence proposed in reaction (1) to explain the mechanism below 432 K.

The observed formation of $CF_3C(O)F$ at higher temperatures can be also rationalized by the quantum chemical calculations. In fact, when the thermal energy of reactants increases, higher vibrational levels of C_4F_8O are populated, so that the unimolecular exit channel leading $CF_3C(O)F$ and the singlet state of the biradical CF_3CF is certainly more favoured. The efficiency of this channel is determined by the interplay established between the collisional stabilization of the highly vibrationally excited PFBE and intramolecular processes leading to $CF_3C(O)F$ molecule and CF_3CF: biradical. In addition, Table 3 shows that the B3LYP, B97-2 and O3LYP functionals predict small electronic barriers of 0.2–3.3 kcal mol^{-1} for the reverse $CF_3C(O)F + CF_3CF$ association, while the B1B95 and B98 methods suggest a simple bond fission (barrierless) process. Our results for the decomposition of thermalized PFBE are in agreement with previous ones calculated at a lower level of theory. In fact, employing the pure functional BPW91/cc-pVDZ, a barrier high of 52.1 kcal mol^{-1} has been reported [44]. As shown in Table 3, our computed values are comprised between 51.2 and 59.8 kcal mol^{-1}.

In summary, the present work shows that the principal products of the reaction between C_4F_8-2 and NO_2 below 432 K are PFBE and NO, and indicates that CF_3CF biradicals are generated by thermal decomposition of PFBE above

this temperature. This system provides a new synthetic method that can produce PFBE with high efficiency. The thermal decomposition of substituted epoxides to generate perfluoroalkylcarbenes is expected to be useful to produce synthetic and biological macromolecules and polymers analogously to the difluorocarbene [14, 15]. The presented DFT calculations support the experimental findings and allow predicting the energetics of the reaction pathways of the reaction mechanism.

Acknowledgement

This research project was supported by the Universidad Nacional de La Plata, the Consejo Nacional de Investigaciones Científicas y Técnicas (CONICET) (PIP 5777), the Comisión de Investigaciones Científicas de la Provincia de Buenos Aires (CICPBA) and the Max Planck Institute for Biophysical Chemistry Göttingen through the "Partner Group for Chlorofluorocarbons in the Atmosphere".

References

1. D. D. Coffman, M. S. Raasch, G. W. Rigby, P. L. Barrick, and W. E. Hanford, J. Org. Chem. **14** (1949) 747.
2. R. N. Haszeldine, J. Chem. Soc. (1953) 2075.
3. D. A. Barr and R. N. Haszeldine, J. Chem. Soc. (1960) 1151.
4. E. R. Bissel, J. Org. Chem. **26** (1961) 5100.
5. I. L. Knunyants, A. V. Fokin, and V. A. Komarov, Zh. Vses. Khim. Obshchestva im. D. I. Mendeleeva **7** (1962) 709.
6. I. L. Knunyants, A. V. Fokin, and V. A. Komarov, Izv. Akad. Nauk, Ser. Khim. **3** (1966) 466.
7. A. V. Fokin and A. T. Uzun, Z. Obshchei Khimii. **36** (1966) 117.
8. B. L. Dyatkin, E. P. Mochalina, and I. L. Knunyants, Russian Chem. Rev. **35** (1966) 417.
9. Ch. W. Spicer and J. Heicklen, Int. J. Chem. Kinet. **4** (1972) 575.
10. R. M. Romano and J. Czarnowski, Z. Phys. Chem. **219** (2005) 849.
11. R. M. Romano, C. O. Della Vedova, and J. Czarnowski, Z. Phys. Chem. **216** (2002) 1203.
12. J. Czarnowski and H. J. Schumacher, Int. J. Chem. Kinet. **18** (1986) 907.
13. R. M. Romano and J. Czarnowski, Z. Phys. Chem. **218** (2004) 575.
14. P. Krusic, D. Christopher Roe, and B. E. Smart, Israel J. Chem. **39** (1999) 117.
15. W. Mahler and P. R. Resnick, J. Fluor. Chem. **3** (1973/74) 451.
16. E. I. Du Pont de Nemours and Co, British Patent 904 877 (1962).
17. D. Chow, M. H. Jones, M. P. Thorne, and E. C. Wong, Can. J. Chem. **47** (1969) 2491.
18. J. Czarnowski, J. Fluor. Chem. **127** (2006) 736.
19. J. Pacansky, R. L. Waltman, and Y. Ellinger, J. Phys. Chem. **98** (1994) 4787.
20. G. D. Bent, E. Zerrad, G. W. Trucks, K. Wiberg, and L. Taing, J. Phys. Chem. **104** (2000) 370.
21. J. Czarnowski, Bull. Polish Akad. Sciences, Chem. **39** (1991) 49.

22. V. Arce, M. dos Santos Afonso, R. M. Romano, and J. Czarnowski, J. Argent. Chem. Soc. **93** (2005) 123.
23. R. M. Romano, C. O. Della Védova, and J. Czarnowski, Int. J. Chem. Kinet. **35** (2003) 532.
24. K. G. Sharp and T. D. Coyle, Inorg. Chem. **11** (1972) 1259.
25. S. Andreades, J. Org. Chem. **27** (1962) 4163.
26. I. P. Kolenko, T. I. Filyakova, A. Y. Zapevalov, and E. P. Lure, Izvest. Akad. Nauk SSSR, Ser. Khim. **11** (1979) 2509.
27. A. D. Becke, Phys. Rev. A **38** (1988) 3098.
28. C. Lee, W. Yang, and R. G. Parr, Phys. Rev. B **37** (1988) 785.
29. M. J. Frisch, J. A. Pople, and J. S. Binkley, J. Chem. Phys. **80** (1984) 3265 and references therein.
30. A. P. Scott and L. Radom, J. Chem. Phys. **100** (1996) 16502.
31. C. J. Cobos, J. Mol. Struct. (Theochem) **581** (2002) 17.
32. M. E. Tucceri, M. P. Badenes, and C. J. Cobos, J. Fluor. Chem. **116** (2002) 135.
33. J. E. Sicre and C. J. Cobos, J. Mol. Struct. (Theochem) **620** (2003) 215.
34. M. P. Badenes, A. E. Croce, and C. J. Cobos, Phys. Chem Chem. Phys. **6** (2004) 747.
35. C. J. Cobos, J. Mol. Struct. (Theochem) **714** (2005) 147.
36. H. L. Schmider and A. D. Becke, J. Chem. Phys. **108** (1998) 9624.
37. P. J. Wilson, T. J. Bradley, and D. J. Tozer, J. Chem. Phys. **115** (2001) 9233.
38. A. D. Becke, J. Chem. Phys. **104** (1996) 1040.
39. W.-M. Hoe, A. J. Cohen, and N. C. Handy, Chem. Phys. Lett. **341** (2001) 319.
40. A. G. Baboul, L. A. Curtiss, P. C. Redfern, and K. Raghavachari, J. Chem. Phys. **110** (1999) 7650.
41. L. A. Curtiss, P. C. Redfern, V. Rassolov, G. Kedziora, and J. A. Pople, J. Chem. Phys. **114** (2001) 9287.
42. M. J. Frisch, G. W. Trucks, H. B. Schlegel, G. E. Scuseria, M. A. Robb, J. R. Cheeseman, J. A. Montgomery, Jr., T. Vreven, K. N. Kudin, J. C. Burant, J. M. Millam, S. S. Iyengar, J. Tomasi, V. Barone, B. Mennucci, M. Cossi, G. Scalmani, N. Rega, G.A. Petersson, H. Nakatsuji, M. Hada, M. Ehara, K. Toyota, R. Fukuda, J. Hasegawa, M. Ishida, T. Nakajima, Y. Honda, O. Kitao, H. Nakai, M. Klene, X. Li, J. E. Knox, H. P. Hratchian, J. B. Cross, C. Adamo, J. Jaramillo, R. Gomperts, R. E. Stratmann, O. Yazyev, A. J. Austin, R. Cammi, C. Pomelli, J. W. Ochterski, P. Y. Ayala, K. Morokuma, G. A. Voth, P. Salvador, J. J. Dannenberg, V. G. Zakrzewski, S. Dapprich, A. D. Daniels, M. C. Strain, O. Farkas, D. K. Malick, A. D. Rabuck, K. Raghavachari, J. B. Foresman, J. V. Ortiz, Q. Cui, A. G. Baboul, S. Clifford, J. Cioslowski, B. B. Stefanov, G. Liu, A. Liashenko, P. Piskorz, I. Komaromi, R. L. Martin, D. J. Fox, T. Keith, M. A. Al-Laham, C. Y. Peng, A. Nanayakkara, M. Challacombe, P. M. W. Gill, B. Johnson, W. Chen, M. W. Wong, C. Gonzalez, and J. A. Pople, Gaussian 03, Revision C.02, Gaussian, Inc., Pittsburgh PA (2004).
43. P. Hohenberg and W. Kohn, Phys. Rev. **136** (1964) B864.
44. C. J. Cramer and M. Hillmyer, J. Org. Chem. **64** (1999) 4850.